



## Optimizing Visibility of Historical Structures Using Modified Weighted Differential Evolution: Insights from the Kromni Valley, Gümüşhane, Türkiye

Mehmet Akif Günen<sup>\*1</sup>, Kaşif Furkan Öztürk<sup>2</sup>, Şener Aliyazıcıoğlu<sup>3</sup>

<sup>1</sup> Gümüşhane University, Department of Geomatics Engineering, Türkiye, akif@gumushane.edu.tr

<sup>2</sup> Gümüşhane University, Department of Civil Engineering, Türkiye, kasiffurkan.ozturk@gumushane.edu.tr

<sup>3</sup> Gümüşhane University, Department of Mining Engineering, Türkiye, s.aliyazicioglu@gumushane.edu.tr

Cite this study: Günen, M. A., Öztürk, K. F., & Aliyazıcıoğlu, Ş. (2025). Optimizing visibility of historical structures using modified weighted differential evolution: Insights from the Kromni Valley, Gümüşhane, Türkiye. *International Journal of Engineering and Geosciences*, 10 (1), 107-126.

<https://doi.org/10.26833/ijeg.1529351>

### Keywords

Kromni valley  
Viewshed  
Historical Structure  
Weighted Differential  
Evolution

### Abstract

It is very important for historical structures to see each other in order to reveal the historical and cultural identity of a region. Historical structures in the Kromni Valley of Gümüşhane, located near the Sümela Monastery, served as places of worship, communication, trade, and social activity centers during their period of active use. This study analyses the spatial relationships of 38 historic buildings, including churches, chapels and castles, whose 3D models are created by in-situ measurements and point clouds obtained by unmanned aerial vehicles, using a 3D viewshed analysis using geographic information systems and remote sensing data. The research introduces a modified weighted differential evolution-based viewshed analysis (mWDE-WS) to enhance the visibility of these structures. In order to assess the applicability of the proposed method, a statistical comparison was conducted between four different Differential Evolution (DE) algorithms (standard DE, LSHADE, CobiDE, JADE and WDE) and the mWDE. The Wilcoxon signed-rank test indicates that mWDE is a more effective solution than alternative methods for addressing the relevant real-world issues. The study also integrates drainage network analysis to assess flood risks and the relationship between cultural structures and water flow. Findings show that historical structures in the region were built not randomly but within a rational approach and 64% of the study area is visible from structures and 2% of the area is visible from ten or more structures. mWDE-WS analysis revealed that the visible area could increase by 20% to 84.37% if the historic structures were placed in optimal locations. In addition, the historical structures were built away from 3rd order streams to minimize flood risk and humidity, demonstrating the community's awareness of the local topography and hydrology.

### Research Article

Received:07.08.2024  
Revised: 16.10.2024  
Accepted:30.10.2024  
Published:01.02.2025



## 1. Introduction

Historical structures are an important part of the identity and the history of a city. They are important sources of information not only for their aesthetic value but also for understanding past lifestyles and architectural techniques. The strategic importance of visibility between historic structures has played a crucial role in the development of architecture and society throughout the history of the city. Preservation of cultural heritage, religious and social interaction, strategic placement and tourism are among the various factors that have indicated important roles in the

settlement and planning of such structures. Modern tools, such as Geographic Information Systems (GIS) and Remote Sensing (RS) technologies, play a crucial role in the conservation, understanding, and management of cultural heritages [1-9]. Visibility analysis has been used in numerous scientific fields for over a half-century, and it has become a standard procedure in assessing and analyzing visual experiences. The literature uses a variety of terminology, including isovist, visualscape, viewshed, and line-of-sight, which may lead to conflicting interpretations. The term "viewshed" is preferred for this investigation. Viewshed often refers to the region seen

from a specific point, although it can also be interpreted as a feature of openness [10]. There is no study in the literature that investigates the purpose of the establishment of a settlement as in this study.

Ogburn proposed a fuzzy viewshed approach modified to take into account target size and emphasized that this method can easily be applicable for GIS-based viewshed analysis [11]. Baek and Choi compared the performance of 2D Fresnel zone, 3D Fresnel zone and line-of-sight analyses to obtain communication viewsheds using high-resolution topographic data for open pit-mine [12]. Researchers showed that when calculating communication potential using different digital surface model resolutions, accurate and reasonable of the 3D Fresnel zone analysis results increased using higher resolution topographical data. By using long-term satellite images, the damages caused by human activities and natural disasters on historical areas can be observed. In this context, Negula et al. focused on risk identification for hazards such as industrialization, erosion and infrastructure work in the Micia and Germisara archaeological sites in Romania, using a multi-temporal Sentinel-2 dataset [13]. Researchers remarked that Sentinel-2 spatial resolution is appropriate for supporting archaeological research and it makes possible to accurately monitor sites and identify potential hazards. These studies create a critical bridge between archaeology and environmental sciences, highlighting the potential of modern technology for the preservation of historic sites and management of archaeological sites. Nowadays, the methods and scope of historical research have changed considerably as technology has advanced. Beck et al., showed Corona and Ikonos imagery for the project Settlement and Landscape Development in the Homs Region, Syria and emphasized that the strategic application of satellite imagery for targeted ground surveys has resulted in cost benefits and better understanding archaeological records [14]. Bridgwood et al. presented a method which automates the discovery of lost or unknown archaeological sites in Egypt by using shape detection on satellite imagery within a GIS framework [15]. Gillings proposed the analytical methods to analyze invisibility, concealment and hiding, based on GIS-based viewshed calculations using a group of visually underwhelming prehistoric stone settings [16]. Results of the research showed that GIS-based viewshed calculations can be investigated and analyzed not only visibility but also invisibility, concealment and seclusion using enough viewsheds and a theoretically sensitive approach. Sánchez-Pardo et al. explored the reasons behind the distribution of the early medieval churches for a Mariña region in North-west Spain using formal analysis of topographic parametrics and showed that the locations of the investigated churches were preferred to provide visual and territorial control on some areas of landscape [17]. Wang and Dou proposed a fast Candidate Viewpoints Filtering algorithm for multi-viewpoint site planning revealing viewpoint optimization selection and compared efficiency of this method with the Region Partitioning for Filtering and Simulated Annealing algorithms [18]. Prus et al. performed the landmark visibility analysis for locations of the structures in area of Carpathian Foothills

in southern Poland using the field of landscape architecture, spatial planning and the use of GIS technology [19]. The examples considered by researchers demonstrate how historical structures are referenced in modern development layouts and how the emergence of new settlement tissue is shaped by cultural context and geographical markers. Bachagha et al. investigated ancient sites in Southern Tunisia. Researchers combined high-resolution remote sensing imagery with on-site investigations to identify potential archaeological sites using satellite data [20]. Riso et al. examined the newly discovered San Nicola church in Sicily and the built settled landscape around it [21]. In the light of methods based on field survey and landscape archaeology, researchers emphasized that San Nicola church can be defined as a landmark church depending on settlement patterns and possible road networks. Doneous et al. proposed a solution that combines an interactive GIS-based archaeological interpretation with a stratigraphic sequence known as a Harris Matrix, extended by an interval-based hierarchical time model [22]. Polat introduces a novel approach aiming to identify potential neolithic sites contemporary with Göbeklitepe in the Southeast Anatolia region [23]. Using visibility maps and the presence of cisterns near known neolithic sites, the study identifies nine potential neolithic sites, offering a framework that can be applied to discover new neolithic areas and enhance our understanding of the neolithic period in similar regions. Braşoveanu et al. investigated the GIS-based surface characterization of 200 ashmound structures for 21 archaeological sites within the help of Airborne Laser Scanning and aerial photography techniques in Romania [24]. In addition, researchers emphasized that ashmound structures have relatively different shapes and the micro relief changes due to the erosion intensity. Civicioğlu and Beşdok investigated various meta-heuristic techniques to find the best possible observation point on a topographic landscape. This point would provide the most extensive viewable area, based on data from the ASTER Digital Terrain Model [25]. Such research plays an important role in preserving historical structures and transferring them to future generations. In this context, advancing historical research in the balance between technology and cultural context can help to understand and preserve historical sites more deeply.

Other researchers discussed water management and stream networks in historical places [26-30]. These studies aim to explore and analyze historical water management and stream networks using modern techniques. They investigate ancient systems for managing flash floods, assess the efficiency of digital terrain models for estimating surface flow and sediment loading, perform quantitative drainage morphometric analyses to compare flow velocities in different watersheds, examine historical water storage capacities as strategic resources. These efforts reveal insights into how ancient civilizations managed water resources and how modern technology can enhance our understanding of these historical practices. Historical structures were constructed to serve various purposes depending on the topography and geographical conditions in which they were built. In the situation that less written and/or

evidentiary documents regarding the purpose for which these structures were built, revealing them scientifically is crucial for the protection of historical and cultural heritage. Geo-spatial analyses are important tools that enable us to learn more about cultural heritage structures and provide effective strategies for their transfer to future generations.

In this study, spatial data of 38 historical structures in Gümüşhane Kromni Valley were collected through in-situ measurements and unmanned aerial vehicle flights to be analyzed by operating both a social and scientific process. To the best of our knowledge, there is no study that includes a detailed analysis of the Kromni Valley using a combination of different methods such as 3D viewshed and hydrological analyses. For the 3D Viewshed analysis, the evolutionary-based WDE method was modified and presented to the literature. In this context, the study is both a scientific and social research. This research integrates various advanced analyses to highlight the significance of the region and aligns with the evolving methodologies in historical research by bridging geography and engineering sciences. The study employed 3D viewshed analysis to determine the visibility of historical structures from their locations, answering questions about where and how much of these structures can be seen. A mWDE-WS was introduced to optimize the placement of cultural structures, ensuring they are visible from more areas when situated in optimal locations, thus maximizing their field of view. This innovative approach contributes a new methodology to the literature. Additionally, four different DE algorithm variants were compared with the mWDE to evaluate the proposed method's applicability. Drainage network analysis was performed to assess the positioning of cultural structures in relation to flood risk and their impact on water flow, integrating hydrological considerations into the spatial analysis. The study scientifically demonstrated that the structures in the Kromni Valley were not placed randomly but followed a deliberate social and scientific hierarchy, reflecting an advanced understanding of landscape and resource management in historical contexts. This comprehensive approach underscores the interdisciplinary nature of modern historical research, combining insights from technological, geographical, and engineering perspectives to deepen our understanding of past civilizations.

## 2. Material and Methods

It is necessary to make positionally precise decisions or to examine fields of view under certain conditions. GIS is an area of information technology used to collect, store, analyze, organize and visualize geographic data. These systems enable geographic data to be represented in

visual formats such as maps and graphs [31]. It also offers user-friendly tools to analyze geographic data and make decisions. Spatial-based analysis is a process that requires processing geographical data. Elevation data, aspect, slope and other geographical information are generally used for these analyzes. Additionally, GIS can be used to integrate analysis results with other geographic data [32, 33]. To perform various analyses of the data, a Digital Surface Model (DSM) with a 5 m grid spacing and high-resolution aerial photographs, created by the Turkish General Directorate of Mapping using the automatic matching method from stereo aerial images with a spatial resolution of 30 cm, were used [34]. Geomax Zenith 15 GNSS receiver was used to determine the locations of historical structures with in-situ measurement. DJI Phantom 4 unmanned aircraft vehicle is used for creating point cloud from aerial images. QGIS 3.28.0 open-source software was used for data integration and data management operations. Viewshed and mWDE-WS analyses were performed with the code prepared in MATLAB 2023a. All these processes are performed on MSI Delta 15 laptop with AMD Ryzen 9 9500 HX processor, RX6700 graphics card, and 32 Gb RAM.

### 2.1. Study area

This study was carried out in the Kromni Valley, which is located approximately 40 km north side of Gümüşhane, Türkiye, hosts various societies and has a 3rd degree archaeological site. The Greek churches and monasteries in the region were abandoned and turned into ruins due to lack of maintenance. The Muslim population living in the Kromni Valley increased and the demographic structure of the region changed. The fact that being not enough research in the literature about the Kromni Valley is the biggest factor in choosing this region. Thus, the region has a long-standing background. The region generally consists of mountains and deep valleys. There are three residential area dominating the region: Yağlıdere, Olucak and Uğurtaş. In the study area, there are 36 historical structures registered by the Ministry of Culture and Tourism, which were originally built as churches or chapels, and 2 castles. Location map and spatial distribution of these structures are presented in Figure 1. In Figure 1, it is seen that the minimum and maximum elevation difference is more than 1000 m. When Figure 1 is examined, as a first impression, according to structure layout, it is seen that historical structures are built upstream instead of downstream where there are more bifurcations. By this way, both visibility is increased and it is positioned related to drainage networks. Turkish National Reference Framework with ITRF96 datum (EPSG:5257) was used for geotagging of aerial images and DSM data.

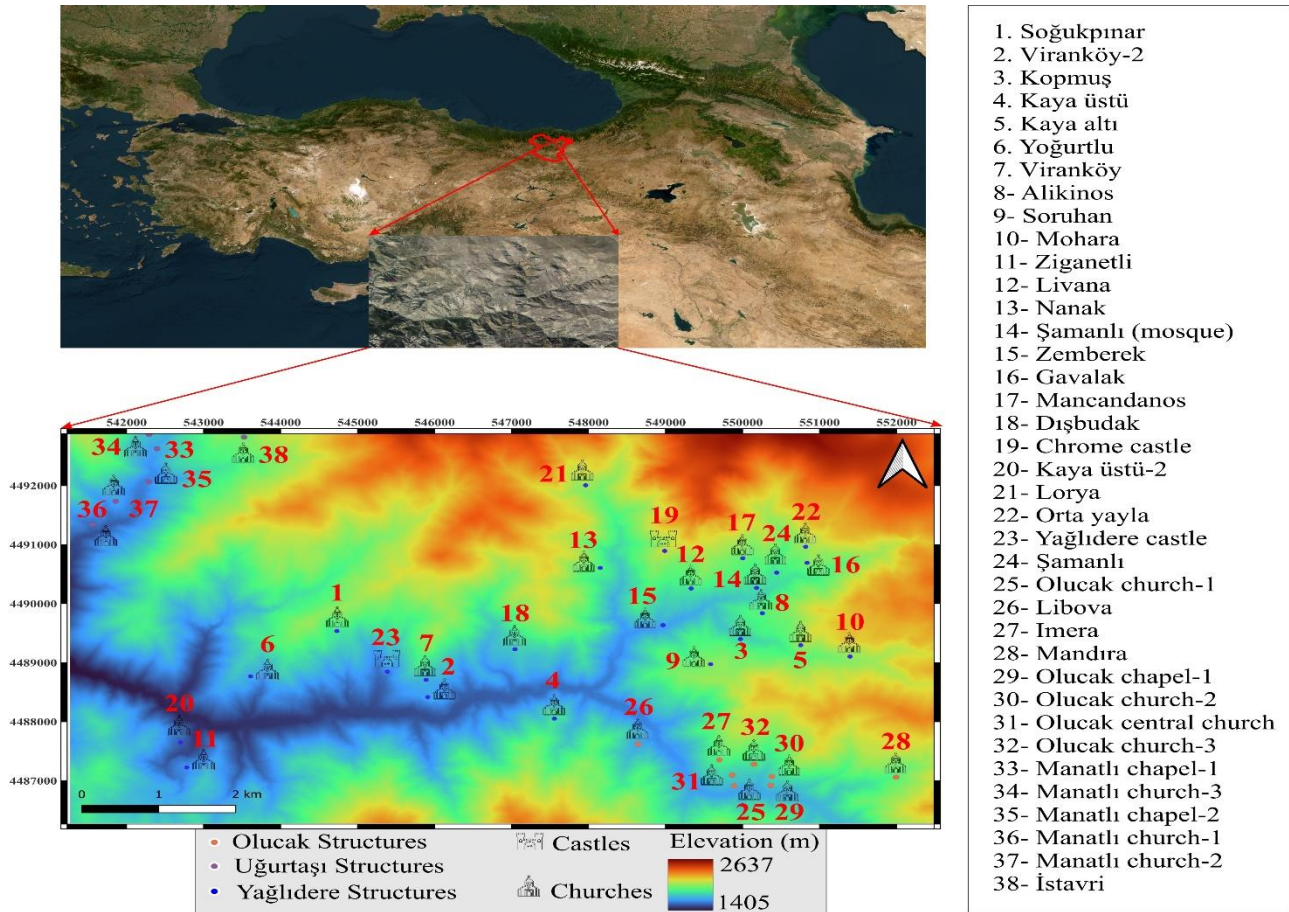
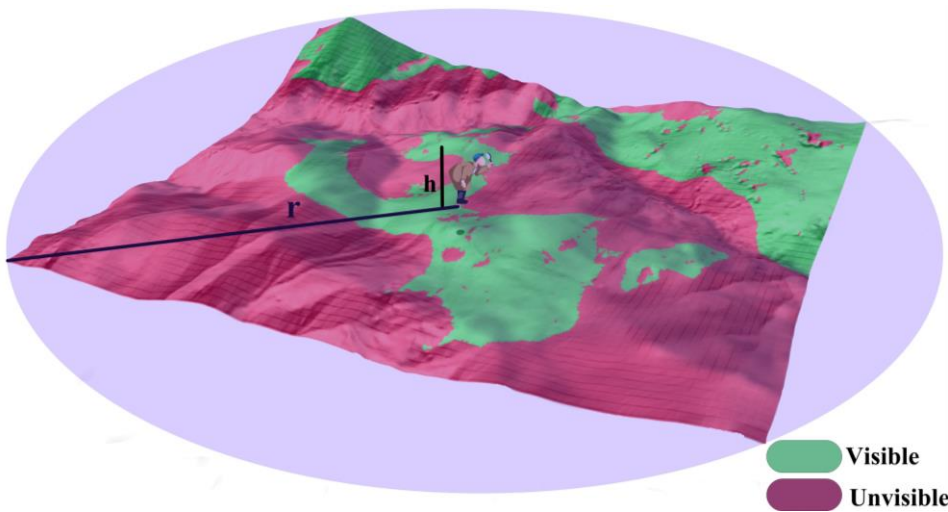


Figure 1. Location map of Kromni valley

## 2.2. Viewshed analysis

Visibility, which can be expressed with the concepts of looking and seeing, forms the basis of surface survey studies in landscape-based cultural heritage research, which is combined in many different ways, from simple to complex. The concept of visibility, in terms of past settlements, civilizations or inhabitants, refers to the ability to see settlements, places of worship, watchtowers, castles and various monuments and artifacts of a past culture from a certain observer position that can be considered significant. Mapping visible regions, visual connection networks and statistically revealing observed phenomena in order to try to explain past spatial choices logically and scientifically are possible with viewshed analysis. Determining the visible areas around cultural structures with viewshed analysis; it can be used to provide important information for the protection of these structures, understanding their construction purposes and revitalizing regional tourism. Furthermore, through viewshed analysis these structures can be better understood and the consciousness values of previous communities can be

appreciated [25, 35-38]. It is used in a number of applications such as 3D viewshed analysis [39], unmanned aerial vehicle (UAV) path planning [40, 41], communication tower positioning [42], sensor coverage optimization [43]. Traditionally, 3D field of view analysis is based on the line-of-sight method, which is obtained from an observation point to all available regions. This analysis is used to visualize the area up to a certain distance from the observer point. There are two basic parameters: observer height ( $h$ ) and viewing distance ( $r$ ). The observer height parameter represents the height of the observer. Usually this refers to the height of where the observer is standing or sitting. This height represents the observer's height above the ground surface in meters. The viewing distance parameter determines how far away the observer can see objects. Viewing range is usually expressed as a unit of angle or distance. Increasing the size of the grid representing the topography makes problem solving difficult and complex. The general view of the 3D viewshed analysis is given in Figure 2.



**Figure 2.** General representation of 3D Viewshed analysis

### 2.3. mWDE-WS

WDE is a variant of the DE optimization algorithm, which is a popular and powerful heuristic algorithm for solving optimization problems. DE is commonly used for global optimization in various fields, including engineering, machine learning and operations research. WDE introduces the concept of weights to modify the selection step. In traditional DE, the selection is based solely on the objective function, where solutions with lower objective function values are preferred. However, in WDE, each solution in the population is assigned a weight, and the selection is performed based on both the objective function value and the weight. The weights can be used to bias the selection towards specific solutions or regions of the search space. Solutions with higher weights are more likely to be selected, which can help guide the search toward certain areas of interest or avoid areas with poor solutions. This allows for a more customized and flexible search strategy [44-46]. In this paper, the efficiency of the WDE algorithm was increased by modifying the trial vector (in Equation 10). The basic steps of WDE are presented below. Equation 1 can be used to define the initial population,  $P$ , of the WDE.

$$P_{(i0,j0)} \sim \mathbf{U}(\text{low}_{(j0)}, \text{up}_{(j0)}) \mid \begin{pmatrix} 2 \cdot N, & D \\ \text{rows} & \text{columns} \end{pmatrix} \leftarrow \text{size}(P) \quad (1)$$

Where,  $i0 = [1:2N]$ ,  $j0 = [1:D]$ ,  $i0, j0 \in \mathbb{N}^+$ ,  $N$  and  $D$  represent the number of pattern vectors and the size of the problem, respectively,  $\text{low}_{j0}$  and  $\text{up}_{j0}$  are lower and upper search limits, respectively.  $\mathbf{U}(\cdot)$  is a continuous uniform distribution. To define the objective function  $\mathcal{F}$ , the objective function value,  $P_{i0}$ , is obtained by Equation 2.

$$\text{fit}P_{(i0)} = \mathcal{F}(P_{(i0)}) \quad (2)$$

In the initial stage of the selection process,  $\text{Sub}P$  is generated from  $P$ . In each iteration, the  $N$  pattern

vectors,  $\text{Sub}P$ , are randomly selected from the set  $P$ , where  $\text{Sub}P$  is defined by the Equation 3.

$$\text{Sub}P = P_{(k)} \mid \{k = j_{(1:N)} \mid j = \text{permute}(1:2N)\} \quad (3)$$

$$\text{Where } \begin{pmatrix} N, & D \\ \text{rows} & \text{columns} \end{pmatrix} \leftarrow \text{size}(\text{Sub}P) \text{ and } \text{permute}(\cdot)$$

denotes the vector permuting function. Objective function values,  $\text{fitSub}P$ , of  $\text{Sub}P$  vectors have been selected from  $\text{fit}P$ , using Equation 4.

$$\text{fitSub}P = \text{fit}P_{(k)} \quad (4)$$

Novel pattern vectors,  $\text{Temp}P$ , is generated in the mutation process.  $\text{Temp}P_{\text{index}=1:N} = \begin{bmatrix} \text{Temp}P_1 \\ \dots \\ \text{Temp}P_N \end{bmatrix}$  vector is reconstructed at each iteration with Equation 5.

$$\text{Temp}P_{(\text{index})} = \sum (w \circ P_{(l)}) \mid l = j \setminus k \quad (5)$$

Where,  $\text{index} = 1:N$ ,  $w^* = \kappa_{(N)}^3 \mid [N,1] = \text{size}(w^*)$ ,  $w^* := \frac{w^*}{\sum w^*}$ ;  $w = w^* \times \Delta$  and  $\Delta = [1]_{(1,D)}$ . Equation 6 is used to update the  $M_{(1:N,1:D)} = 0$  matrix, which manages the random crossover process throughout each iteration.

$$M_{(\text{index},J)} := 1 \quad (6)$$

Where,  $J = V(1:\lceil K \times D \rceil) \mid V = \text{permute}(j0)$  and “:=” represents updating operator. The conditioned-rule in Equation 7 defines  $K$ .

$$\text{If } \alpha < \beta \text{ then } K = \kappa_{(1)}^3 \text{ else } K = (1 - \kappa_{(1)}^3) \quad (7)$$

In Equation 7,  $\alpha, \beta, \kappa \sim U(0,1)$ ,  $(\cdot) = size(\kappa_{(\cdot)})$ . At each call of  $\kappa_{(\cdot)}$ , it produces a new set of real-valued uniform  $(\cdot)$  sized random numbers. Equation 8 provides the conditioned rule that is used in WDE to generate the numerical value of the evolutionary step size, also known as the scale factor.

$$F = \begin{cases} [\lambda_{(D)}^3] & \text{if } \alpha < \beta, \quad size(F) = [1, D] \\ \lambda_{(N)}^3 \times \Delta & \text{else,} \quad size(F) = [N, D] \end{cases} \quad (8)$$

Equation 9 is used to produce the trial vector, T, and  $T \notin [low \ up]$  values are updated using Equation 10.

$$T = SubP + F \times M \circ (TempP - SubP_{(m)}) \quad | \quad m = permute(i) | m \neq [1 : N] \quad (9)$$

Here,  $i = 1 : N | i \in Z^+$ . In the mWDE trial vector is updated using Equation 10.

$$T = T + \kappa \circ randi([0 \ 1], N) \circ (gbest - T) \quad (Eq. 15 \text{ for } gbest) \quad (10)$$

At each call, *randi* creates a new, randomly generated, integer-valued matrix in the interval [0 1], consisting of N rows and 1 column. Equation 11 is utilized in updating  $T \notin [low \ up]$  values.

$$\begin{cases} \text{if } (T_{(i,j0)} < low_{(j0)}) \text{ then } T_{(i,j0)} = low_{(j0)} + \kappa_{(1)}^3 (up_{(j0)} - low_{(j0)}) \\ \text{if } (T_{(i,j0)} > up_{(j0)}) \text{ then } T_{(i,j0)} = up_{(j0)} + \kappa_{(1)}^3 (low_{(j0)} - up_{(j0)}) \end{cases} \quad (11)$$

Equation 12 is used to generate the objective function values of the T vectors.

$$fitT = \mathcal{F}(T) \quad (12)$$

Using T and *fitT*, *SubP* and *fitSubP* are updated in accordance with the greedy-selection rule. The conditioned rule found in Equation 13 is used during the update phase.

$$\begin{aligned} & \text{if } (fitT_{(i^*)} < fitSubP_{(i^*)}) \\ & \text{then } [SubP_{(i^*)}, fitSubP_{(i^*)}] := [T_{(i^*)}, fitT_{(i^*)}] \quad | \quad i^* \in i \end{aligned} \quad (13)$$

$P_{(l)}$  and  $fitP_{(l)}$  values are updated using updated *SubP* and *fitSubP*. Equation 14 has the required updating phase provided.

$$[P_{(l)}, fitP_{(l)}] := [SubP, fitSubP] \quad (14)$$

Finally, Equation 15 is used to generate the global solution vector, *gbest*, of WDE.

$$[gmin, gbest] = [fitP_{(\gamma)}, P_{(\gamma)}] \quad | \quad fitP_{(\gamma)} = \min(fitP) \quad , \quad \gamma \in i \quad (15)$$

Gridded DSM data was used to perform WDE-based 3D viewshed analysis. Here, each cell of the topographic grid,  $T(i,j)$ , is labeled 0 and 1 depending on whether it is visible or not. The objective function is defined by Equation 16, with the grid dimensions *uy* and *ux*.

$$\arg \min \frac{\sum T | T == 0}{uy \times ux} \quad (16)$$

## 2.4. Comparison methods

In this paper, WDE, mWDE and four different DE variants are statistically compared for solving the WS problem. In order to handle nonlinear issues, Price and Storn created DE Algorithm, a population-based stochastic search algorithm, in 1995 [47]. The reason behind its creation was the lack of effectiveness of Genetic Algorithms (GA) in parameter optimization for practical issues. DE uses the same operators as GA - mutation, crossover, and selection- but in a different way. In order to produce new people through crossover and mutation, three different chromosomes are selected at random from the population. Newly created chromosomes from the application of these operators are passed on to the following generation if their fitness values are higher than those of their predecessors. DE can be readily stuck in local solutions and frequently shows unstable convergence behavior despite its straightforward and widely understood structure. The algorithm's ability to solve intricate, multimodal, and closely connected numerical problems is limited by the use of fixed-value parameters for scale and crossover factors. Because there is no analytical model for the best mutation and crossover tactics, DE must rely on laborious trial-and-error procedures to find appropriate parameters. In order to improve resilience and get around the drawbacks of the conventional DE algorithm, more advanced mutation and crossover models have been added to contemporary DE versions. These models frequently contain random processes [45, 46, 48].

DE algorithm with Linear Population Size Reduction (LSHADE), an extension of Success History-Based Adaptive DE, is a linear population size reduction method intended to improve performance in large-scale optimization tasks. This method begins with a larger population, enabling a thorough investigation of the search space. The population is progressively reduced throughout the course of subsequent generations in order to concentrate more on optimizing and utilizing the best solutions discovered. This reduction strategy expedites convergence while lowering processing requirements. LSHADE improves scalability and performance in complex optimization problems by balancing exploration and exploitation [25, 44, 49].

DE based-on Covariance Matrix Learning and Bimodal Distribution Parameter Setting (COBIDE) is

presented as an extended version of DE. It incorporates more complex methods for maintaining population variability and parameter fitting. The main novelty is the use of covariance matrix learning. This technique allows the algorithm to adapt to the geometry of the fitness landscape. In addition, COBIDE uses a bimodal distribution parameterization method for setting mutation and crossover values. This method uses Cauchy distributions with predefined parameters. The values are generated with a 50% probability, increasing the robustness and adaptability of the algorithm. As a result, COBIDE is able to handle complex optimization problems with greater ease. This approach promotes successful convergence while preserving the diversity of the population [25, 48, 50].

Adaptive DE with optional external archive (JADE), an improved variant of DE, is described as using an optional external archive and the DE/current-to-best mutation approach to achieve maximum performance. The DE/current-to-best technique, by focusing solely on the optimal solution, can lead to premature convergence. In contrast, JADE's strategy incorporates a range of top solutions. This strategy maintains diversity and achieves a balance between exploration and exploitation by using insights from a wider range of recently discovered effective solutions. Research has shown that JADE is highly effective, often outperforming other DE variants due to its flexible methodology and the advantageous use of an archive to guide the search process [25, 48, 51].

## 2.5. Drainage network

Drainage network refers to the road system used in GIS and hydrology fields where the water of a region is naturally collected and separated. Drainage network describes the movement of rainfall water on the surface, an organization in which streams and rivulets combine to form large rivers and eventually flow into the sea or oceans. Drainage network analyses are used in a number of hydrological and environmental applications, such as water resources management [52], flood forecasting [53], water quality monitoring [54] and geographic planning [55]. Rivers and streams in a geographical area allow water to flow in a certain direction. Larger rivers can be formed from the points where these streams combined. A drainage network includes all flow channels flowing from a given reference point to another point. The network is limited by a topographically defined grid structure. A drainage network begins with first-order streams to which no other streams are connected. In the most used flow sequence method, a second-order flow begins where the first-order flow meets, a third-order flow begins where two second-order flows meet, and so on [56-58].

## 3. Results and Discussion

Kromni Valley is located in a geography with higher than 1000 meters, in the transition zone of Black Sea and Continental climates, hot and dry in summers and cold

and rainy in winters. There are abundant mineral reserves in this region, and the ores found in Kromni and Imera mining areas generally contain copper, lead, zinc, gold and silver. During the Ottoman Empire period, the control of the mines in the region was of strategic importance within the scope of expansion policies. There are different theories about the name of this region; it is claimed that the name "Kurum" mentioned in the Ottoman Empire records is a settlement belonging to the Turkmen society named Göklen [59]. According to Bilgin [60], the name Kurum was used as the name of a "Hakan" during the Bulgarian Turkic Khanate. According to Andreadis [61], the name "Kromni", given by the Greeks, originated from the density of the rocks in the region, and in time, it led to the Greek name of the people of the region.

Various historical structures in this region, such as caravanserais, bridges, castles and cemeteries, are important elements that shed light on the historical, cultural and economic past of the region. However, comprehensive studies on the topographic features of these structures, their relationships with each other and their interaction with the environment are limited. In this context, three-dimensional visibility analysis of 38 historical structures was conducted using GIS analyses and remote sensing data, and their spatial distributions and visual relationships with each other were examined. In addition, the drainage networks of the regions where historical structures are located will be analyzed and their relationship with the use of water resources and the selection of locations will be investigated. These analyses will contribute to a better understanding of the historical structures in the Gümüşhane Kromni Valley, the development of conservation strategies and the evaluation of the archaeological potential of the region. The historical structures discussed in this study served as centers of communication, trade and social activities during the period of their active use. The visual connectivity of these structures facilitated communication and interaction between communities and contributed to the integration and development of societies. In addition, the fact that these structures could see each other enabled effective observation and defense strategies and increased the security of settlements. From a religious perspective, the fact that historical structures built at critical points can see each other symbolizes the ties and unity between believers. This facilitates the organization of religious gatherings and ceremonies and strengthens the spiritual significance of these places in the society. Furthermore, the strategic placement of structures at key points allows them to serve as landmarks for travelers and pilgrims, attracting visitors and contributing to the economic and cultural vitality of the region.

Figure 3 shows the number of structures whose visible areas intersect as a result of the viewshed analysis performed using the high-resolution DSM of the study area, and the spatial distribution of these structures on the 3D terrain model for visual interpretation.

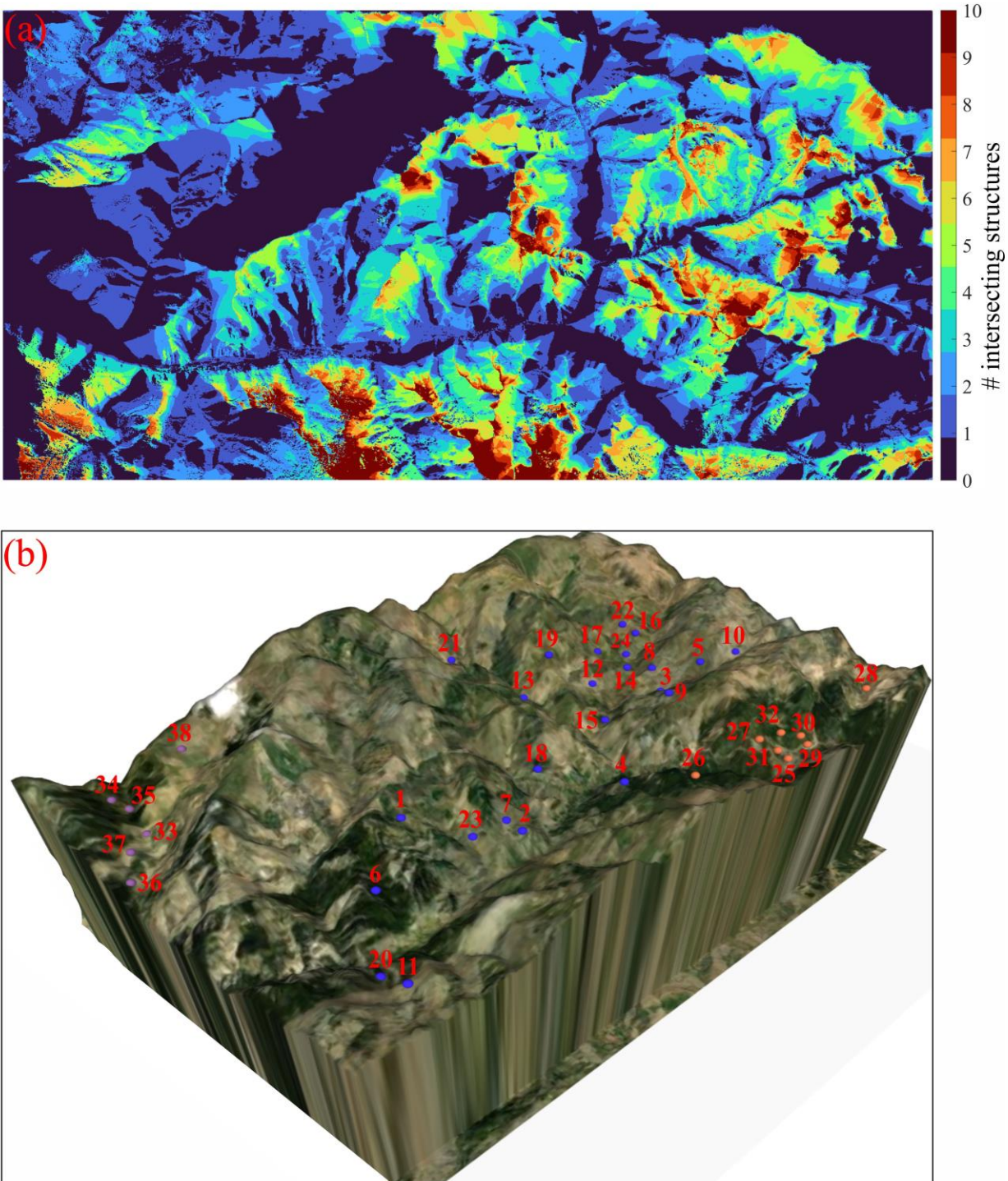


**Figure 3.** (a) Intersection areas of structures and (b) 3D presentation by overlaying DSM and aerial photography

Figure 3.a shows the spatial distribution of the land surfaces where the dark blue areas are not visible at all (not visible to historic structures) and the red scale shows the spatial distribution of the land surfaces where 10 or more historic structures can see each other. The north-east and north-west regions of the study area are generally the least visible areas in terms of structures. Both on-site observations and remote sensing images made in this region did not reveal any ruins in the region. Among the reasons for the absence of structures in these regions, it is considered that there is no construction against avalanche threat due to the steep topographical structure and heavy snow. When Figure 3-b is analyzed, it is determined that these areas are topographically hilly

and obstruct the visibility angle and no historical structures or ruins were found in these regions. In general, it was observed that historical structures were built close to the settlement centers of Uğurtaş, Olucak and Yağlıdere villages shown in Figure 1.

The analysis was carried out to determine whether the historical structures can see each other in a point-centered approach. In this context, the intersection point of the roof axes of the historic structures gives the average height of the structures. The visibility lines obtained as a result of the visibility analysis performed by adding 1.7 m (accepted as the average human height) to structure height, are presented in Figure 4.

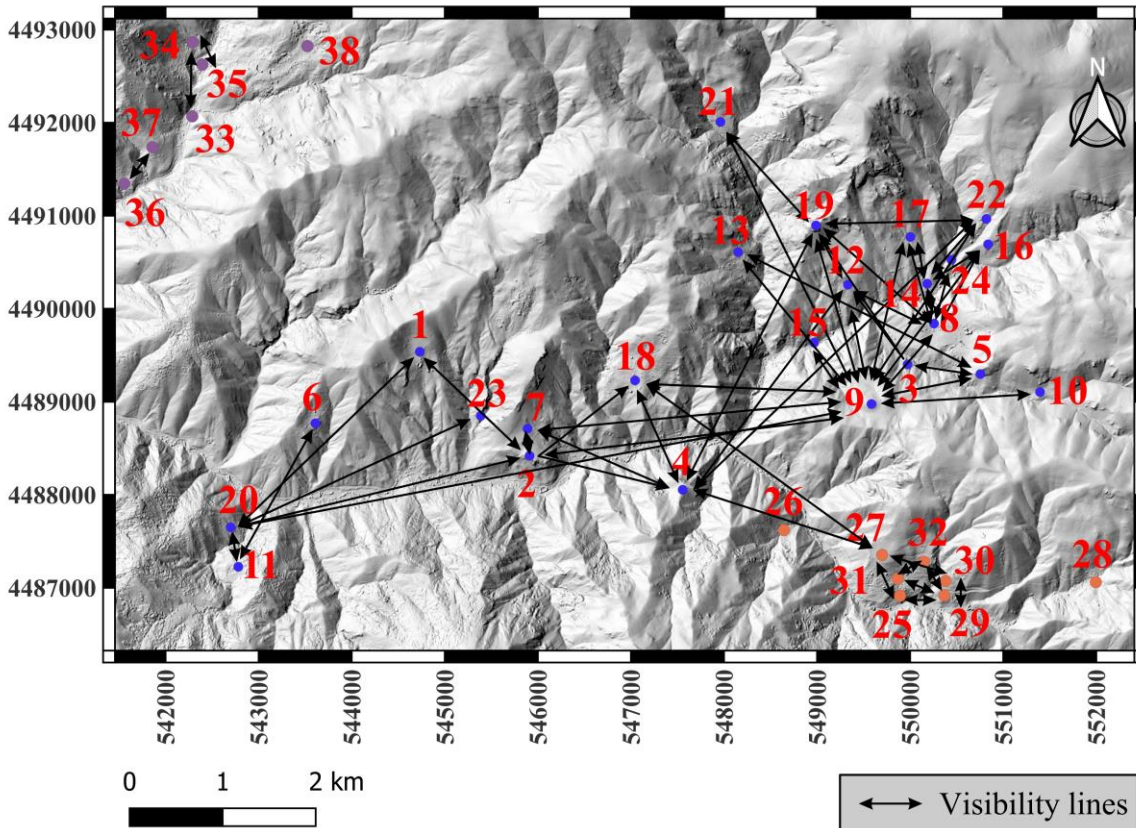


**Figure 4.** Visibility lines between churches

In Figure 4, the direction of the arrow indicates the direction seen by the observer. The opposite direction represents what is seen. According to the flow lines or valleys of the stream, the settlement was planned in accordance with the topography and not on the stream flow lines. The analysis revealed that the Soruhan church (number 9) is the most seen structure, while Madira church (number 28) and

Istavri church (number 38) are the least seen structures. In this context, it is thought that the structure Soruhan church was built on the dominant hill and was the center of religious rituals performed in the region. It is important to realize the spatial analysis of each individual historic structure in relation to the study area. In this scope, the intersection of church visibility area is presented in Figure 5.

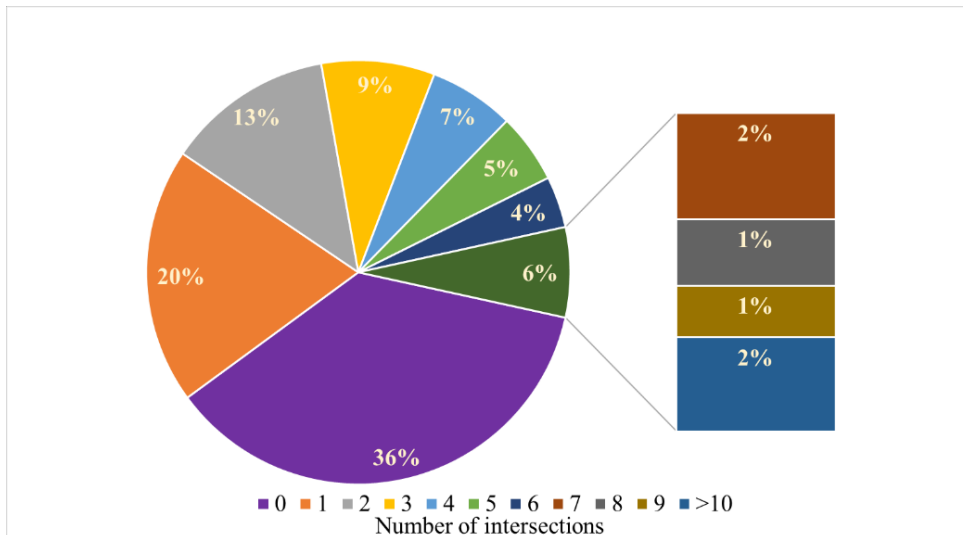


**Figure 5.** Illustration of intersections of church visibility areas.

When Figure 5 is analyzed, it is determined that approximately 64% of the total area in the study area is seen by the structures. It is revealed that approximately 2% of these areas can be seen by 10 or more structures, and the total of the areas seen individually can be seen by a single structure in a total of 20% of the total area.

Determining the visibility of each structure in relation to the total area in the study area is critical for the individual examination of the structures. Within this context, the visibility rate of each individual structure relative to the total area is given in Figure 6.

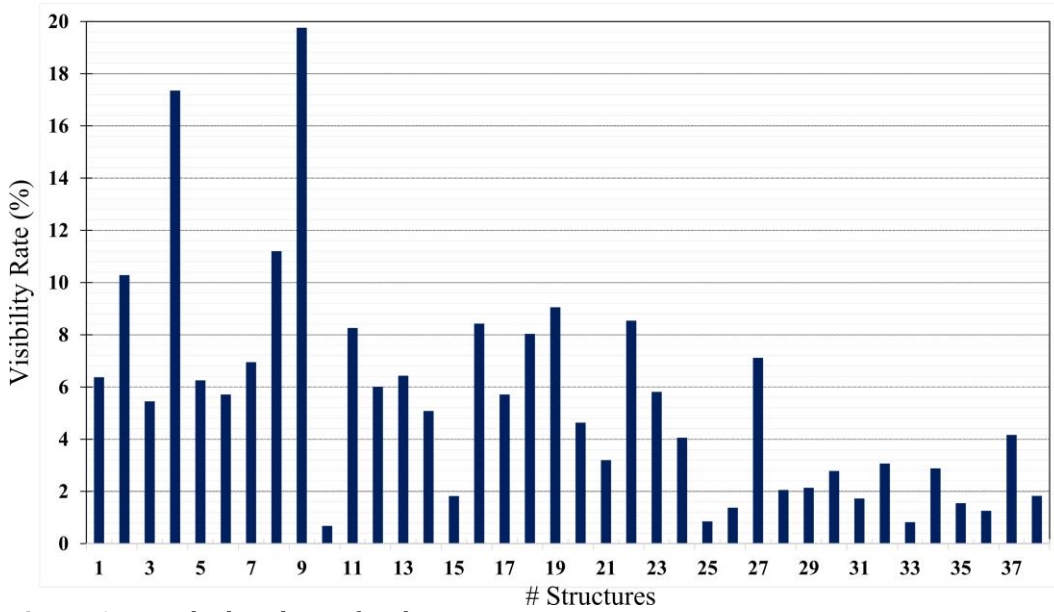


**Figure 6.** Viewshed analysis of each structure

Kayaüstü (numbered 4) and Soruhan (numbered 9) churches have the highest visibility of the study area, while Mohara (numbered 10) and Olucak church-1 (numbered 25) churches have the lowest visibility. 3D model created by using unmanned aerial vehicle images of Soruhan, Kayaalti, and Mohara Churches is presented in Figure 7. When the relevant figures are examined, it is

seen that Soruhan Church is built on a dominant hill and has the ability to see the region, while Kayaalti Church has limited visibility as one side faces the mountain. As can be seen from here, the church was built on a dominant hill. Visibility of each structure on DSM data is given in Figure 8.

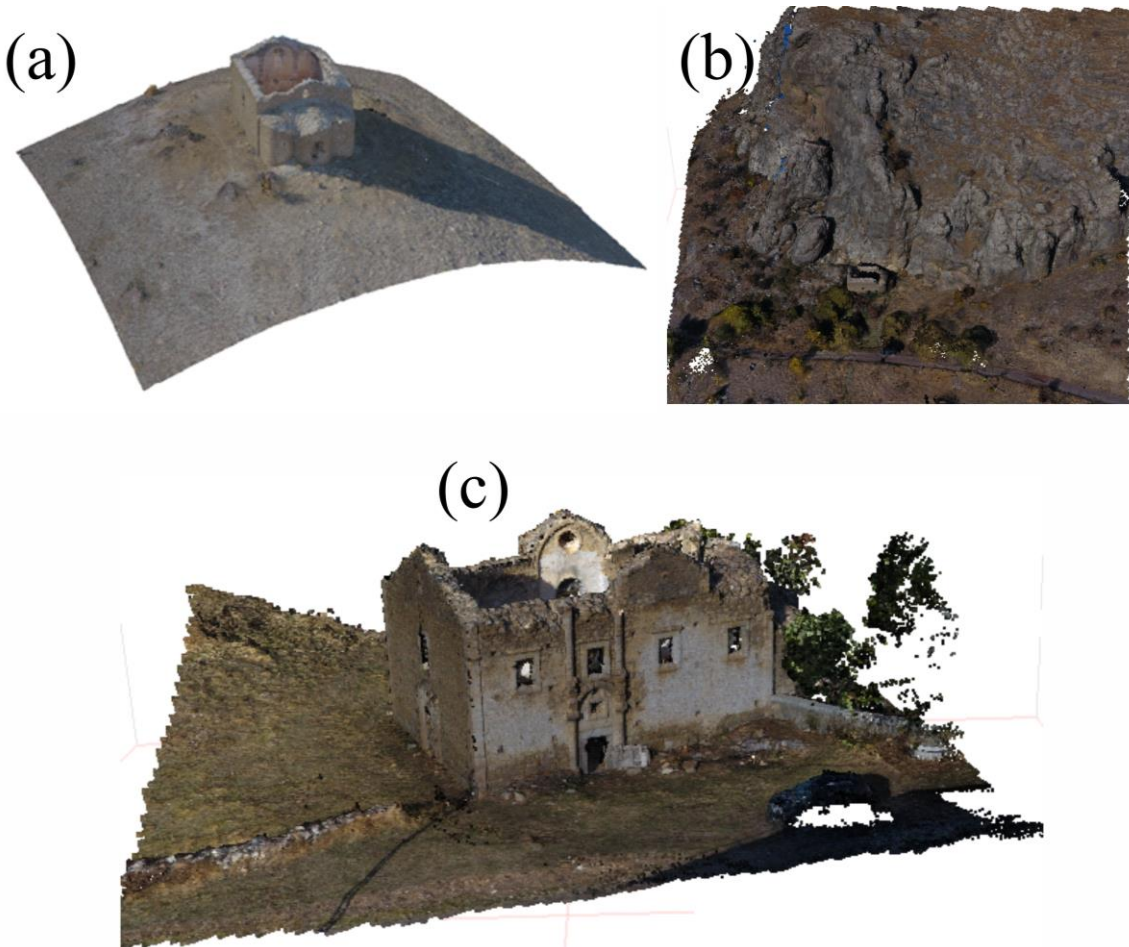


**Figure 7.** 3D model of a) Soruhan, b) Kayaalti, and c) Mohara Churches.

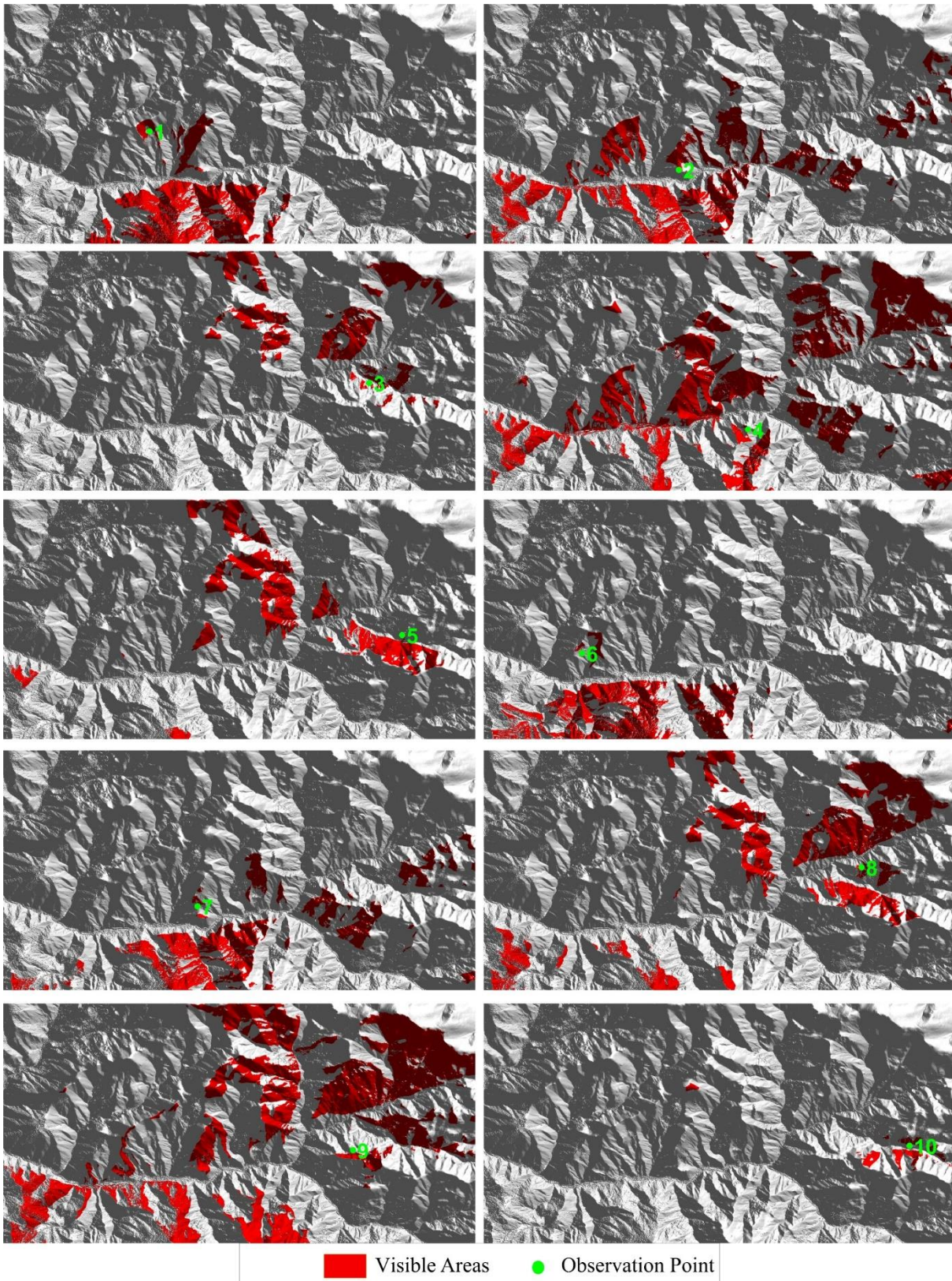


**Figure 8.** Visibility of each observation point

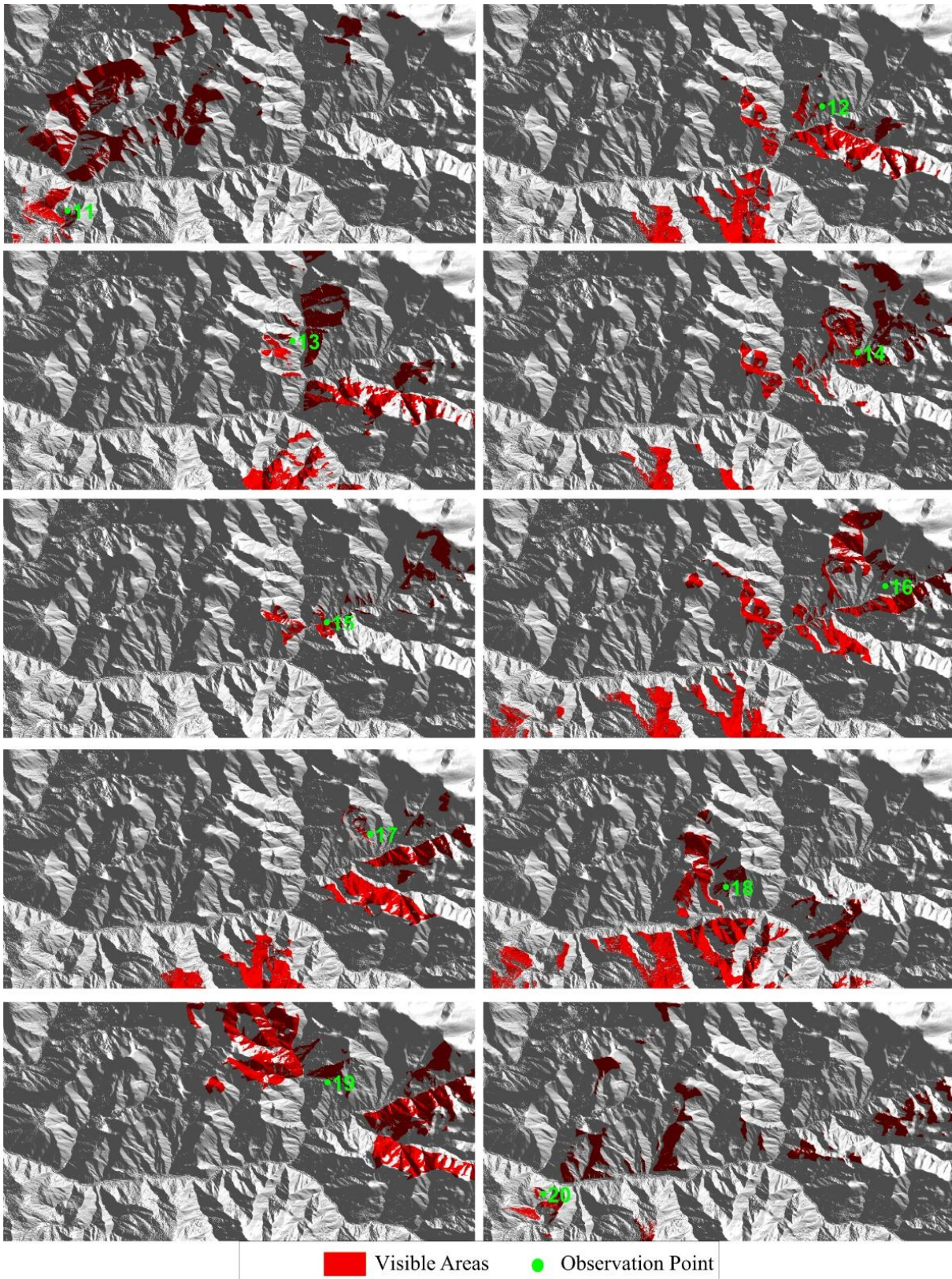
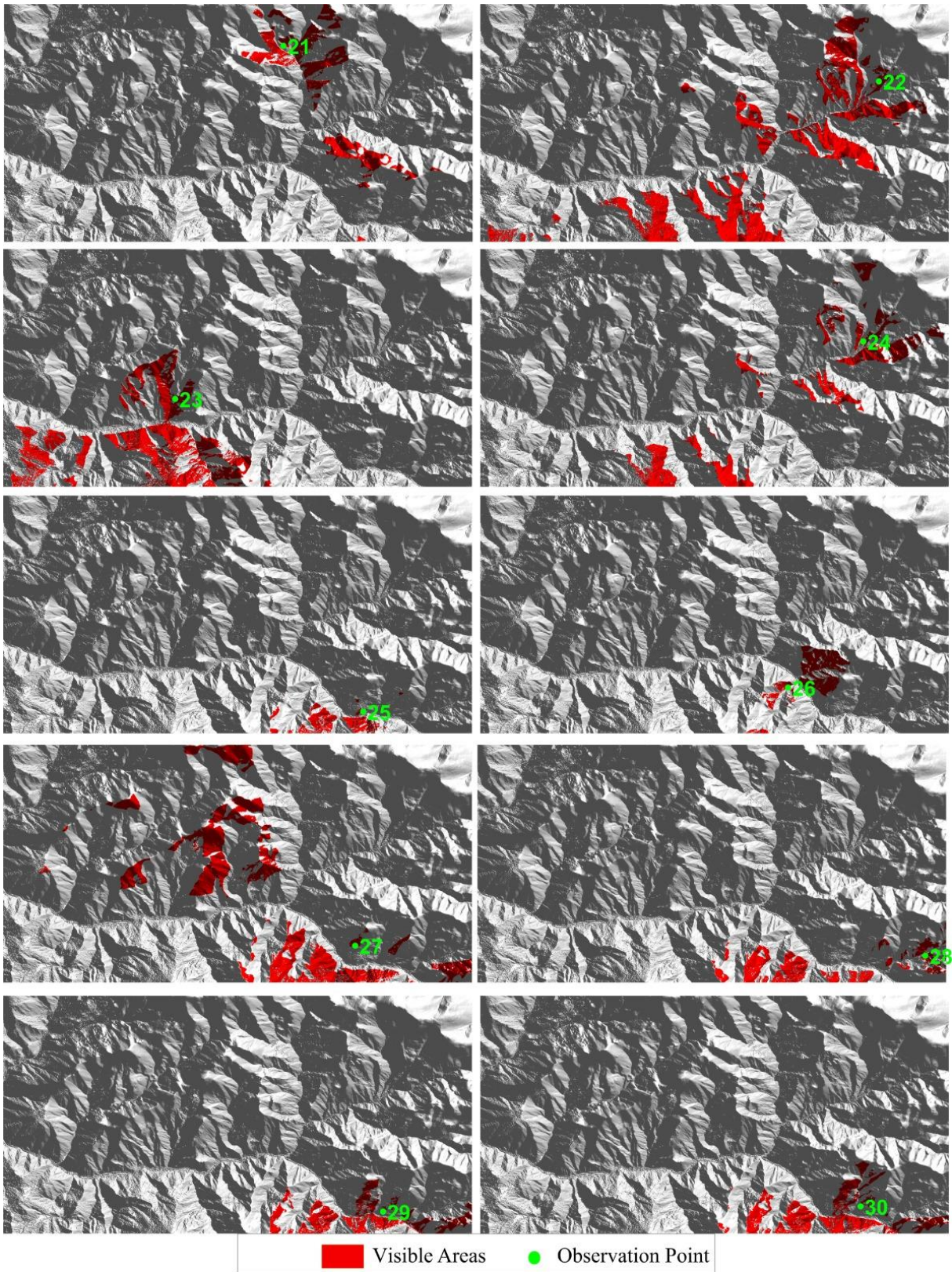
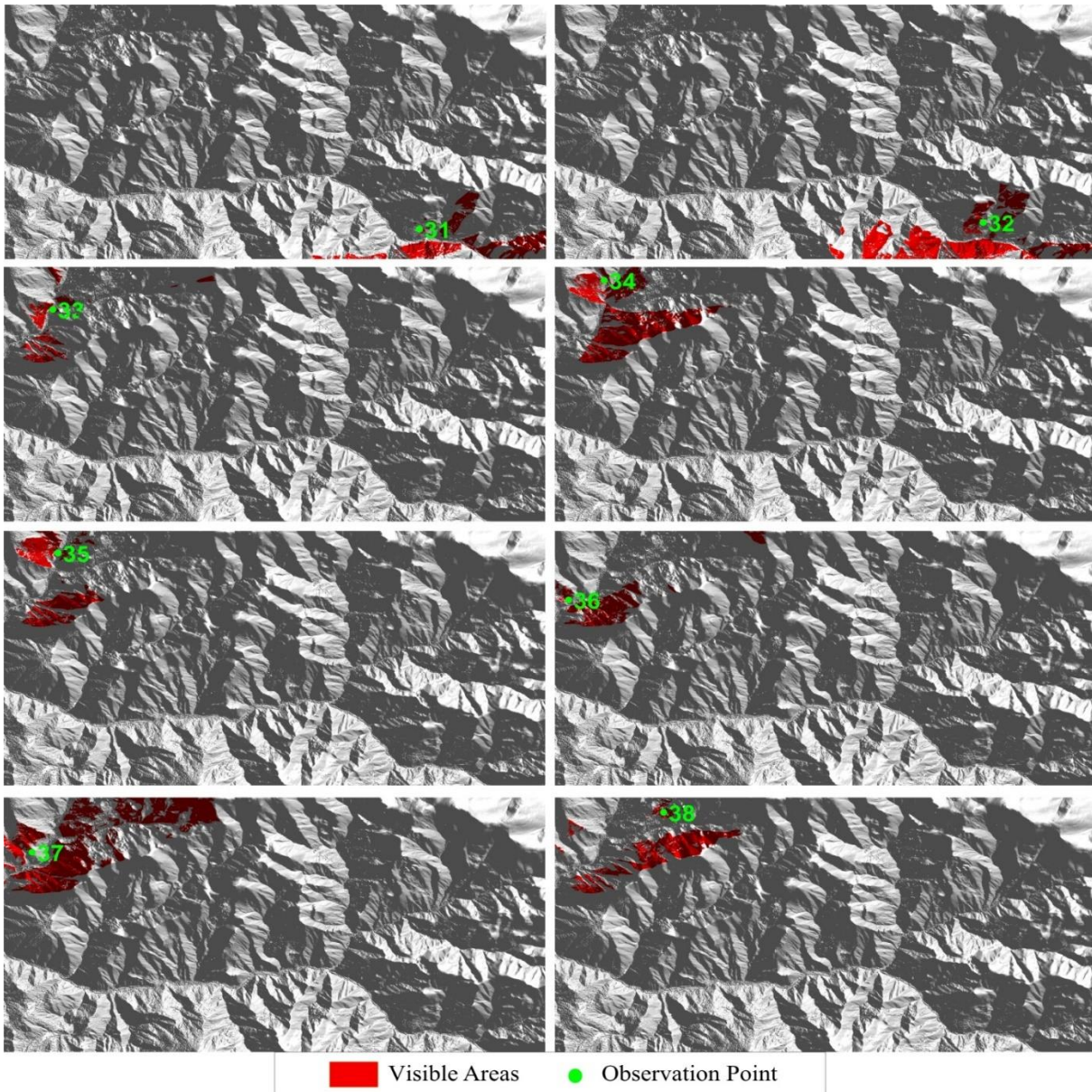


Figure 8 (continued). Visibility of each observation point



**Figure 8** (continued). Visibility of each observation point



**Figure 8** (continued). Visibility of each observation point

Optimal positioning is the process of placing a structure or facility in an optimal and strategic way to achieve specific objectives. This process requires consideration of many different factors and usually involves a number of criteria such as cost savings, efficiency, accessibility, safety and environmental impacts. For every method utilized in the experiments, population matrix size and the maximum iteration number were consistently set at 20 and 10,000, respectively. Each test function was addressed through thirty tries, each initiated with a different initial population. Table 1 outlines the internal parameters of the comparison methods. The pertinent references provide the control parameters for the comparison methods. The mWDE does not have a control parameter like WDE. Only the value for the number of populations needs to be adjusted. A grid search was conducted by increasing the number of populations by 10 within the range of 10-100, and the value of 20, which provided the best result, was used.

**Table 1.** Control parameters of comparison methods

| Method          | Parameters  |
|-----------------|---|
| CobiDE [25, 62] | $F \sim N(\mu c; 0.1); CR \sim Cauchy(\mu c; 0.1);$<br>$c = 0.1; p = 0.05$    |
| JaDE [63]       | $\beta = 1.5; p_0 = 0.25$   |
| DE [64]         | $Cr = 0.9; F = 0.5$   |
| LshaDE [25, 62] | $p_{best\ rate} = 0.11; arcrate = 1.4; memory\ size = 5;$<br>$minpopsize = 4$ |

Boxplots are a useful instrument for clearly illustrating the median of a data set as well as the distribution and summary statistics of the data. When comparing different data sets or determining whether a given data set is symmetrical or skewed, the median, which represents the central tendency of the data set, can be quite helpful. The box plot is constructed in Figure 9 according to the results given by the objective function values of the relevant methods.

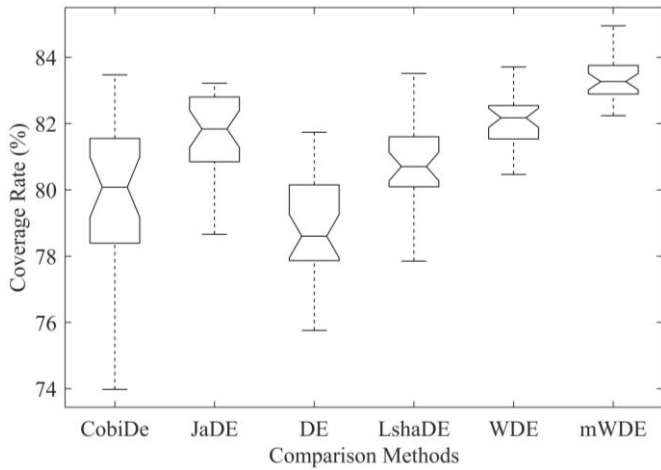


**Figure 9.** Box plot analysis of coverage rate supplied by DE variants.

The narrower distribution and highest median coverage rates of the mWDE, WDE, and JaDE approaches suggest that they are more reliable and effective. The LshaDE method has the lowest median value, at roughly 78%. The distribution of the mWDE and WDE methods is narrower than that of the CobiDe and LshaDE methods. This suggests that while CobiDe and LshaDE yield more inconsistent results, mWDE and WDE methods perform more consistently.

A non-parametric statistical test called the Wilcoxon signed rank test is used to examine the differences between two dependent samples. Since this test yields accurate results even with small sample sizes, it is especially preferred when the normal distribution assumption is disregarded. The test considers the ranks and signs of the data and assesses the difference in the

median between paired data sets. The results of the test are interpreted in terms of the p-value and a decision is made whether to reject the null hypothesis at a given significance. The Wilcoxon signed-rank test with a statistical significance level of  $\alpha=0.05$  was used to evaluate the relative effectiveness of the experimental results of the WS problem supplied by comparison algorithms and mWDE. The results of a Wilcoxon Signed Rank test, which evaluated the coverage rate values obtained by mWDE and comparison methods, are shown in Table 2.

**Table 2.** Statistical comparison of mWDE and other methods using Wilcoxon signed-rank test.

| Method | P value    | Z value | Rank sum | Winner |
|--------|------------|---------|----------|--------|
| CobiDE | 3.1817e-06 | 4.6587  | 459      | +      |
| JaDE   | 4.4493e-05 | 4.0828  | 431      | +      |
| DE     | 1.7344e-06 | 4.7821  | 465      | +      |
| LshaDE | 2.3534e-06 | 4.7204  | 462      | +      |
| mWDE   | 1.6394e-05 | 4.3091  | 442      | +      |

The '+' symbol signifies that mWDE yields statistically better solutions to the 3D viewshed problem compared to the other methods. In this context, mWDE-WS was performed and the capacity of 38 historical structures to see more area in case of optimum location was ensured by means of current technologies. Best solution of mWDE-WS among to 30 tries used for analysis. Within these results, spatial locations that allow 84.37% of the whole area to be seen were used. Thus, if the areas built in the region were built under today's conditions, approximately 20% more area would be seen. The results obtained with mWDE-WS are presented in Figure 10.

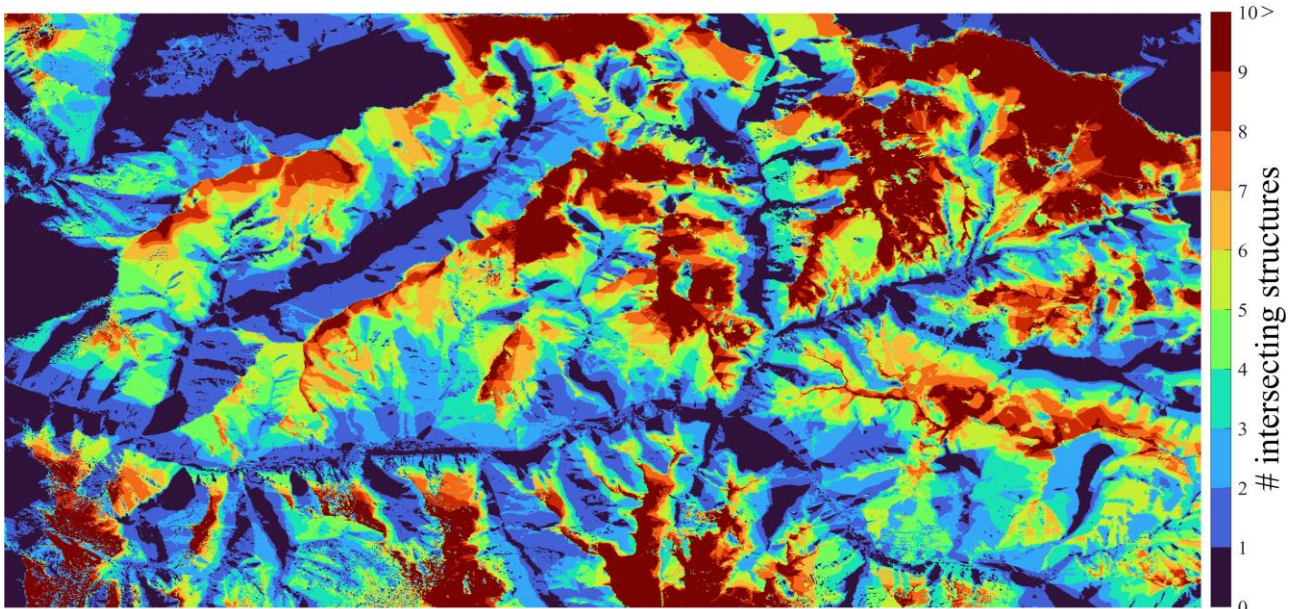


**Figure 10.** Intersected churches result of mWDE-WS

The appropriate positioning of historic structures in water drainage networks provides several important advantages. Firstly, this positioning helps to prevent water erosion. Correct drainage systems allow rainwater to drain away without damaging the structure, protecting its foundation and surroundings. It also reduces the risk of structural damage. Water

accumulation or moisture can weaken the structure of historic structures, but a proper drainage network ensures that water is directed in the right way. This reduces structural damage and increases the durability of the structure. In this context, in order to analyze whether the historical structures in the region are installed according to the drainage networks, the

Strahler Stream Order method [65] was used and super imposed on high-resolution aerial photographs and presented in Figure 11.

When Figure 11 is analyzed in general, it is seen that the settlements were established in such a way that they do not coincide with the stream orders. The smallest and shortest drainage lines are shown as red colored in Figure 11. Typically, it denotes the initial grades at which water gathers and flows into bigger streams. The color yellow denotes drainage lines of moderate size. Usually

created when first order streams converge. The longest and largest drainage lines are shown in green. It holds more water and is created when smaller streams come together. The structures are located away from stream order 3 and close to stream order 1, thus protecting the structures against possible flooding and water risk and humidity. When the detailed areas in the image are examined, it is seen that the drainage networks pass very close to the structures but do not touch the boundaries of the structures.

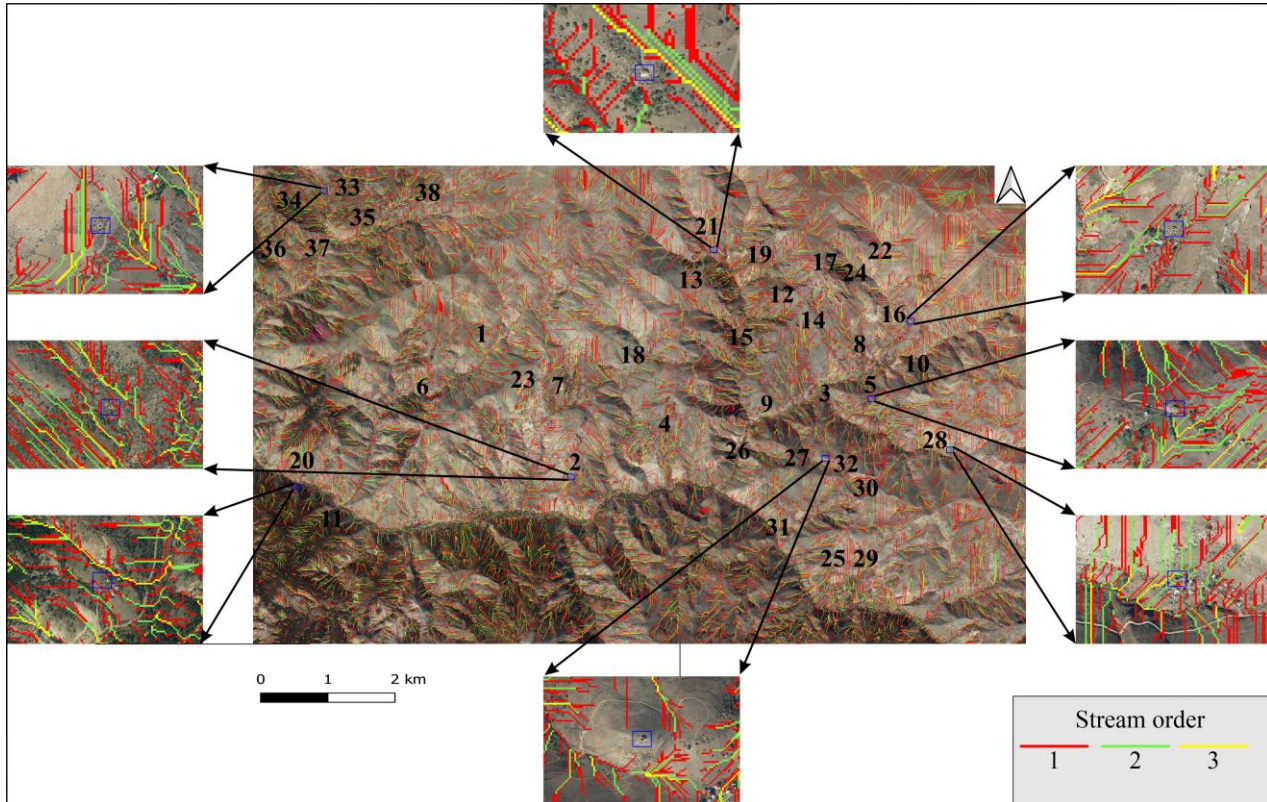


**Figure 11.** Drainage networks of Kromni Valley

#### 4. Conclusions

In conclusion, this study conducted a comprehensive spatial and viewshed analysis of historical structures in the Gümüşhane Kromni Valley, shedding light on the rich history and cultural significance of the region. The 38 historical structures, including churches, chapels, and castles, were examined using three-dimensional viewshed analysis GIS, and remote sensing data. The analysis revealed that 64% of the study area is visible from the historical structures, with 2% being visible from at least 10 structures. By employing a novel mWDE-WS, the potential visibility was increased to 84.37%, indicating that optimal positioning could significantly enhance the visibility of these structures. The mWDE-(WS) algorithm demonstrated significant improvements in optimizing the visibility of historical structures compared to traditional methods such as CobiDE, JaDE, DE, and LshADE. The statistical significance of these findings was confirmed through the Wilcoxon signed-rank test, which highlighted the superior performance of mWDE over other methods. The analysis using the Strahler Stream Order method demonstrated that the historical structures were strategically constructed away from higher-order streams (particularly third-order streams) to mitigate flood risks, water damage, and humidity. This finding suggests that the community possessed a deep understanding of the local topography and hydrology. The analysis provides a comprehensive understanding of the spatial relationships and visual connections between these historical structures. When the strategic importance of historical structures seeing each other is emphasized, the observation terraces to be built in these places and the restoration of these structures will contribute to the revival of regional tourism and the protection of cultural heritage. This will attract tourists' attention, encourage the discovery of idle historical structures in different regions and new tourism destinations may emerge. In addition, the historical and architectural awareness in the region will increase the sense of continuity and interconnectedness and the awareness of the protection of historical structures will increase. In these analyses, DSM resolution can limit the accuracy of both viewshed and drainage networks analysis. Therefore, DSM with high spatial resolution should be used. In addition, the population size and low-up limit values to be chosen in mWDE-WS analysis will change the convergence quality of the algorithm to the problem solution, so it is important to determine these parameters by optimization.

Briefly, it is revealed that mWDE-WS analysis could be more convenient in viewshed analysis of historical places and gives relatively more accurate results compared to other analysis which applied in this study. Also, combining viewshed analysis with drainage networks will lead to optimum site selection. The myth that the churches/chapels and

such structures were built in view of each other among the people of the region, which is the subject of the study, has been scientifically discussed for the first time in this study. In addition, combining the analysis of drainage networks with the visibility analysis, it was revealed that the historical buildings were built not only to see each other but also to avoid coinciding with the waterways.

#### Acknowledgement

Thanks to Republic of Türkiye Ministry of National Defence General Directorate of Mapping and The Scientific and Technological Research Council of Türkiye.

#### Author contributions

**Mehmet Akif Günen:** Writing, Conceptualization, Application of methods  
**Kaşif Furkan Öztürk:** Writing, Research, Editing, Literature search  
**Şener Aliyazıcıoğlu:** Writing, Research, Interpretation and Editing.

#### Conflicts of interest

The authors declare no conflicts of interest.

#### References

1. Bijaber, N., Rochdi, A., Yessef, M., & El Yacoubi, H. (2024). Mapping the structural vulnerability to drought in Morocco. *International Journal of Engineering and Geosciences*, 9(2), 264-280.
2. Ernst, F., Akdağ, S., Polat, N., Akaslan, D., Önal, M., & Ekinci, A. (2024). Development of a virtual reality application for the Old Harran School. *International Journal of Engineering and Geosciences*, 9(1), 77-85.
3. Buhur, S., Uluğtekin, N., Gümüşay, M. Ü., & Musaoğlu, N. (2023). Turistik amaçlı mekânsal sanal ortamların oluşturulması: Tarihi Yarımada Örneği. *Geomatik*, 8(2), 99-106.
4. Yurtsever, A. (2023). Taşınır ve taşınmaz kültür varlıklarının yeni nesil LiDAR sensörlü tablet bilgisayar ile belgelenmesi. *Geomatik*, 8(2), 200-207.
5. Günen, M. A., Kulakoğlu, F., & Besdok, E. (2024). Accuracy assessment of UAV-based documentation of archaeological site: Kültepe-Kaneş. *Digital Applications in Archaeology and Cultural Heritage*, 35, e00380.
6. Silwal, A., Tamang, S. & Adhikari, R. (2022). Use of unmanned aerial vehicle (UAV) for mapping, and accuracy assessment of the orthophoto with and without using GCPs: A case study in Nepal. *Mersin Photogrammetry Journal*, 4(2): p. 45-52.
7. Doğan, Y. & Yakar, M., (2018). GIS and three-dimensional modeling for cultural heritages. *International Journal of Engineering and Geosciences*, 3(2): p. 50-55.

8. Tabakoğlu, C. (2024). A review: detection types and systems in remote sensing. *Advanced GIS*, 4(2): p. 100-105.
9. Fiumi, L. (2023). Remote sensing analysis on Rome's squares. *Advanced Remote Sensing*, 3(2): p. 79-89.
10. Inglis, N. C., Vukomanovic, J., Costanza, J., & Singh, K. K. (2022). From viewsheds to viewscapes: Trends in landscape visibility and visual quality research. *Landscape and Urban Planning*, 224, 104424.
11. Ogburn DE. (2006) Assessing the level of visibility of cultural objects in past landscapes. *Journal of Archaeological Science*. 33:-405-413.
12. Baek, J., & Choi, Y. (2018). Comparison of communication viewsheds derived from high-resolution digital surface models using line-of-sight, 2D Fresnel zone, and 3D Fresnel zone analysis. *ISPRS International Journal of Geo-Information*, 7(8), 322.
13. Dana Negula, I., Moise, C., Lazăr, A. M., Rîșcuța, N. C., Cristescu, C., Dedulescu, A. L., & Badea, A. (2020). Satellite remote sensing for the analysis of the micia and germisara archaeological sites. *Remote Sensing*, 12(12), 2003.
14. Beck, A., Wilkinson, K., & Philip, G. (2007, October). Some techniques for improving the detection of archaeological features from satellite imagery. In *Remote sensing for environmental monitoring, GIS applications, and geology VII* (Vol. 6749, pp. 17-28). SPIE.
15. Bridgwood, I., Rasmussen, M. S., Sørensen, M. K., Carlucci, R., Bernardini, F., & Osman, A. (2007). Automatic detection of archaeological sites using a hybrid process of remote sensing, GIS techniques and a Shape Detection Algorithm. In *ENVISAT Symposium 2007*.
16. Gillings, M. (2015). Mapping invisibility: GIS approaches to the analysis of hiding and seclusion. *Journal of Archaeological Science*, 62, 1-14.
17. Sánchez-Pardo, J. C., Carrero-Pazos, M., Fernández-Ferreiro, M., & Espinosa-Espinosa, D. (2020). Exploring the landscape dimension of the early medieval churches. A case study from A Mariña region (north-west Spain). *Landscape History*, 41(1), 5-28.
18. Wang, Y., & Dou, W. (2020). A fast candidate viewpoints filtering algorithm for multiple viewshed site planning. *International Journal of Geographical Information Science*, 34(3), 448-463.
19. Prus, B., Wilkosz-Mamcarczyk, M., & Salata, T. (2020). Landmarks as cultural heritage assets affecting the distribution of settlements in rural areas—An analysis based on lidar dtm, digital photographs, and historical maps. *Remote sensing*, 12(11), 1778.
20. Bachagha, N., Wang, X., Luo, L., Li, L., Khatteli, H., & Lasaponara, R. (2020). Remote sensing and GIS techniques for reconstructing the military fort system on the Roman boundary (Tunisian section) and identifying archaeological sites. *Remote Sensing of Environment*, 236, 111418.
21. Riso, M., Randazzo, M. G., & Arena, A. E. (2022). Churches at a Crossroads: Assessing a Rural Sacred Landmark in Central Sicily (Sixth to Twelfth Centuries AD). *Landscapes*, 23(2), 103-122.
22. Doneus, M., Neubauer, W., Filzwieser, R., & Sevara, C. (2022). Stratigraphy from topography II. The practical application of the Harris Matrix for the GIS-based spatio-temporal archaeological interpretation of topographical data. *Archaeologia Austriaca*, 106, 223-252.
23. Polat, N. (2023). Utilizing GIS for the exploration of possible neolithic sites contemporary to Göbeklitepe. *Geocarto International*, 38(1), 2240277.
24. Brașoveanu, C., Mișu-Pintilie, A., & Brunchi, R. A. (2023). Inside Late Bronze Age Settlements in NE Romania: GIS-Based Surface Characterization of Ashmound Structures Using Airborne Laser Scanning and Aerial Photography Techniques. *Remote Sensing*, 15(17), 4124.
25. Civicioglu, P., & Besdok, E. (2024). Colony-Based Search Algorithm for numerical optimization. *Applied Soft Computing*, 151, 111162.
26. Abdelal, Q., Al-Rawabdeh, A., Al Qudah, K., Hamarneh, C., & Abu-Jaber, N. (2021). Hydrological assessment and management implications for the ancient Nabataean flood control system in Petra, Jordan. *Journal of Hydrology*, 601, 126583.
27. Hupy, J. P., & Wilson, C. O. (2021). Modeling streamflow and sediment loads with a photogrammetrically derived UAS digital terrain model: Empirical evaluation from a fluvial aggregate excavation operation. *Drones*, 5(1), 20.
28. Ismail, M., Singh, H., Farooq, I., & Yousuf, N. (2022). Quantitative morphometric analysis of Veshav and Rembi Ara watersheds, India, using quantum GIS. *Applied Geomatics*, 14(2), 119-134.
29. Elmakayes, Y., Ben-Shlomo, D., Anker, Y., & Frumkin, A. (2023). Water as a strategic resource in the Western Samaria Region—The Unique Case of Deir Sam'an: the water system that has been operating for 1,500 years. *Environmental Archaeology*, 1-15.
30. Polat, N. (2023). An investigation of ancient water collection and storage systems near the Karahantepe neolithic site using UAV and GIS. *Environmental Archaeology*, 28(6), 475-487.
31. Günen, M. A., Erkan, İ., Aliyazıcıoğlu, Ş., & Kumaş, C. (2023). Investigation of geometric object and indoor mapping capacity of Apple iPhone 12 Pro LiDAR. *Mersin Photogrammetry Journal*, 5(2), 82-89.
32. Yılmaz, H. Ö., & Günen, M. A. (2024). Is environment destiny? Spatial analysis of the relationship between geographic factors and obesity in Türkiye. *International Journal of Environmental Health Research*, 34(3), 1847-1859.

33. Günen, M. A. (2021). Determination of the suitable sites for constructing solar photovoltaic (PV) power plants in Kayseri, Turkey using GIS-based ranking and AHP methods. *Environmental Science and Pollution Research*, 28(40), 57232-57247.
34. Yakar, M., Yilmaz, H. M. & Yurt, K. (2010). The effect of grid resolution in defining terrain surface. *Experimental Techniques*, 34, 23-29.
35. Fisher, P. F. (1993). Algorithm and implementation uncertainty in viewshed analysis. *International Journal of Geographical Information Science*, 7(4), 331-347.
36. Ren, L., & Cao, Y. (2021). GIS-based viewshed analysis on the conservation planning of historic towns: The case study of Xinchang, Shanghai. *The International Archives of the Photogrammetry, Remote Sensing and Spatial Information Sciences*, 46, 609-616.
37. Santosa, H., Yudono, A., Sutikno, F. R., Adhitama, M. S., Tolle, H., & Zuliana, E. (2023). Visibility Evaluation of Historical Landmark Building Using Photographic Survey Coupled with Isovist and Viewshed Analysis. *International Review for Spatial Planning and Sustainable Development*, 11(4), 71-92.
38. De Montis, A., & Caschili, S. (2012). Nuraghes and landscape planning: Coupling viewshed with complex network analysis. *Landscape and Urban Planning*, 105(3), 315-324.
39. Günen, M. A. (2021). Fotogrametrik Nokta bulutunun Görünürlük Analizinde Kullanımı: Gümüşhane Seyir Terası Yer Seçimi. *Avrupa Bilim ve Teknoloji Dergisi*, (28), 295-299.
40. Sanchez-Fernandez, A. J., Romero, L. F., Bandera, G., & Tabik, S. (2021). VPP: visibility-based path planning heuristic for monitoring large regions of complex terrain using a UAV onboard camera. *IEEE Journal of Selected Topics in Applied Earth Observations and Remote Sensing*, 15, 944-955.
41. Hong, X., (2023). The integration of UAV, deep learning, and GIS in the assessment of a new neighborhood concept. *Advanced UAV*. 3(1): p. 1-9.
42. Bharadwaj, S., Dubey, R., Zafar, M. I., Srivastava, A., Bhushan Sharma, V., & Biswas, S. (2020). Determination of optimal location for setting up cell phone tower in city environment using lidar data. *The International Archives of the Photogrammetry, Remote Sensing and Spatial Information Sciences*, 43, 647-654.
43. Han, Z., Li, S., Cui, C., Song, H., Kong, Y., & Qin, F. (2019). Camera planning for area surveillance: A new method for coverage inference and optimization using location-based service data. *Computers, environment and urban systems*, 78, 101396.
44. Pérez-Delgado, M. L., & Günen, M. A. (2023). A comparative study of evolutionary computation and swarm-based methods applied to color quantization. *Expert Systems with Applications*, 231, 120666.
45. Günen, M. A. (2021). Weighted differential evolution algorithm based pansharpening. *International Journal of Remote Sensing*, 42(22), 8468-8491.
46. Civicioglu, P., Besdok, E., Gunen, M. A., & Atasever, U. H. (2020). Weighted differential evolution algorithm for numerical function optimization: a comparative study with cuckoo search, artificial bee colony, adaptive differential evolution, and backtracking search optimization algorithms. *Neural Computing and Applications*, 32, 3923-3937.
47. Yakar, M., Yilmaz, H. M. & Mutluoglu, O. (2010). Close range photogrammetry and robotic total station in volume calculation. *International Journal of the Physical Sciences*. 5(2), 086-096.
48. Gunen, M. A., Besdok, E., Civicioglu, P., & Atasever, U. H. (2020). Camera calibration by using weighted differential evolution algorithm: a comparative study with ABC, PSO, COBIDE, DE, CS, GWO, TLBO, MVMO, FOA, LSHADE, ZHANG and BOUGUET. *Neural Computing and Applications*, 32(23), 17681-17701.
49. Mohamed, A. W., Hadi, A. A., Fattouh, A. M., & Jambi, K. M. (2017, June). LSHADE with semi-parameter adaptation hybrid with CMA-ES for solving CEC 2017 benchmark problems. In 2017 IEEE Congress on evolutionary computation (CEC) (pp. 145-152). IEEE.
50. Wang, Y., Li, H. X., Huang, T., & Li, L. (2014). Differential evolution based on covariance matrix learning and bimodal distribution parameter setting. *Applied Soft Computing*, 18, 232-247.
51. Zhang, J., & Sanderson, A. C. (2009). JADE: adaptive differential evolution with optional external archive. *IEEE Transactions on evolutionary computation*, 13(5), 945-958.
52. Radmehr, A., Bozorg-Haddad, O., & Loáiciga, H. A. (2022). Developing strategies for agricultural water management of large irrigation and drainage networks with fuzzy MCDM. *Water Resources Management*, 36(13), 4885-4912.
53. Piadeh, F., Behzadian, K., & Alani, A. M. (2022). A critical review of real-time modelling of flood forecasting in urban drainage systems. *Journal of Hydrology*, 607, 127476.
54. Yazdi, J. (2018). Water quality monitoring network design for urban drainage systems, an entropy method. *Urban Water Journal*, 15(3), 227-233.
55. Lourenço, I. B., Guimarães, L. F., Alves, M. B., & Miguez, M. G. (2020). Land as a sustainable resource in city planning: The use of open spaces and drainage systems to structure environmental and urban needs. *Journal of Cleaner Production*, 276, 123096.
56. Martz, L. W., & Garbrecht, J. (1992). Numerical definition of drainage network and subcatchment areas from digital elevation models. *Computers & Geosciences*, 18(6), 747-761.
57. Jasiewicz, J., & Metz, M. (2011). A new GRASS GIS toolkit for Hortonian analysis of drainage

- networks. *Computers & Geosciences*, 37(8), 1162-1173.
58. Al-Saady, Y. I., Al-Suhail, Q. A., Al-Tawash, B. S., & Othman, A. A. (2016). Drainage network extraction and morphometric analysis using remote sensing and GIS mapping techniques (Lesser Zab River Basin, Iraq and Iran). *Environmental Earth Sciences*, 75, 1-23.
59. Bostan, M. H. (1993). XV-XVI. Asırlarda Trabzon Sancağında Sosyal ve İktisadi Hayat (Doctoral dissertation, Marmara Üniversitesi (Turkey)).
60. Bilgin, M. (2007). Doğu Karadeniz: tarih, kültür, insan (Vol. 332). Ötüken Neşriyat.
61. Andreadis, Y. (1999). Gizli Din Taşıyanlar, 2. baskı. Belge Yayınları, İstanbul.
62. Civicioglu, P., & Besdok, E. (2021). Bezier Search Differential Evolution Algorithm for numerical function optimization: A comparative study with CRMLSP, MVO, WA, SHADE and LSHADE. *Expert Systems with Applications*, 165, 113875.
63. Civicioglu, P., & Besdok, E. (2023). Bernstein-Levy differential evolution algorithm for numerical function optimization. *Neural Computing and Applications*, 35(9), 6603-6621.
64. Günen M. A. (2021). Evolutionary Computing Based Camera Calibration, Institute of Science, Doctoral thesis: Erciyes University.
65. Strahler, A. N. (1957). Quantitative analysis of watershed geomorphology. *Eos, Transactions American Geophysical Union*, 38(6), 913-920.



© Author(s) 2025. This work is distributed under <https://creativecommons.org/licenses/by-sa/4.0/>